exist and are difficult to identify, but to our knowledge these are not large enough to account for differences between theory and experiment.

It is expected that mean field estimates of molecular interaction are inexact, and we regard the approximate concord between experiment and theory as quite satisfactory. It is not surprising that the parameter v depends slightly on q, even though a strict application of the theory demands that it be independent of q. The results in the tables and figures provide a first estimate of the validity of this theoretical model.

Summary and Conclusions

1. Small-angle neutron scattering studies of polystyrene and its deuterated homologue in deuteriotoluene have been analyzed so that intermolecular and intramolecular contributions are clearly separated. The experiments were performed over a wide concentration range.

2. $S_T(q)$, the total scattering (in the absence of isotopic fluctuations), decreases rapidly with concentration. The ratio $S_T(q)/S_s(q)$ also decreases with increasing concentration, and that decrease is more rapid at low q. The very low values of that ratio at low q are a consequence of the apparent homogeneity of the solution on a scale of q^{-1}.

3. An interaction length, L_i, is defined as that value of q^{-1} at which $S_T(q) = |S_p(q)|$. In these experiments, L_i varies with $c^{-0.73}$. This variation is akin to that found for the screening length ξ, which varies as $c^{-0.70}$. See ref 1.

4. Agreement between the Benoit–Benmouna theory and these experiments is relatively good in the range $0.03 < c < 0.16$. At high concentration, experimental error in $S_T(q)$ is too large to permit a serious test of the theory. At low concentration, discrepancies arise from experimental errors and, perhaps, because molecular overlap is insufficient for the theory to apply.

5. In the Benoit–Benmouna theory, the excluded volume parameter varies with c^n. The experiments yield $0.5 < n < 0.6$. Scaling theory yields a value of n between 0.25 and 0.41, depending on the parameter ν chosen for the relation $R \sim M^\nu$.

Acknowledgment. This work was supported by National Science Foundation Grant No. DMR-8217460.

References and Notes

(1) King, J. S.; Boyer, W.; Wignall, G. D.; Ullman, R. *Macromolecules* **1985**, *18*, 709.
(2) Zimm, B. H. *J. Chem. Phys.* **1948**, *16*, 1093.
(3) Jannink, G.; de Gennes, P.-G. *J. Chem. Phys.* **1968**, *48*, 2260.
(4) Benoit, H.; Benmouna, M. *Polymer* **1984**, *25*, 1059.
(5) Akcasu, A. Z.; Summerfield, G. C.; Jahshan, S. N.; Han, C. C.; Kim, C. Y.; Yu, H. *J. Polym. Sci., Polym. Phys. Ed.* **1980**, *18*, 863.
(6) Benoit, H.; Koberstein, J.; Leibler, L. *Makromol. Chem., Suppl.* **1981**, *4*, 85.
(7) Koehler, W. C.; Hendricks, R. *J. Appl. Phys.* **1979**, *50*, 1951.
(8) Child, H. R.; Spooner, S. J. *J. Appl. Crystallogr.* **1980**, *13*, 259.
(9) des Cloizeaux, J. *J. Phys. (Les Ulis, Fr.)* **1975**, *36*, 281.
(10) Einstein, A. *Ann. Phys. (Leipzig)* **1910**, *33*, 1275.
(11) Debye, P. *J. Appl. Phys.* **1944**, *15*, 338.
(12) Flory, P. J. *J. Chem. Phys.* **1949**, *17*, 303.
(13) LeGillou, J. C.; Zinn-Justin, J. *Phys. Rev. Lett.* **1977**, *39*, 95.
(14) Einaga, Y.; Miyake, Y.; Fujita, H. *J. Polym. Sci., Polym. Phys. Ed.* **1979**, *17*, 2103.

Effects of Polymer Structure and Incorporated Salt Species on Ionic Conductivity of Polymer Complexes Formed by Aliphatic Polyester and Alkali Metal Thiocyanate

Masayoshi Watanabe,* Masahiro Rikukawa, Kohei Sanui, and Naoya Ogata

Department of Chemistry, Sophia University, 7-1 Kioi-cho, Chiyoda-ku, Tokyo 102, Japan.
Received April 17, 1985

ABSTRACT: The effects of polymer structure and incorporated salt species on ionic conductivity were investigated in polymer complexes formed by aliphatic polyester and alkali metal thiocyanate (LiSCN, NaSCN, and KSCN). Poly(ethylene succinate) (PE-2,4) and poly(ethylene sebacate) (PE-2,10) were selected as the host polymers. The incorporated salts were dissolved in the amorphous region of the host polymers. The temperature dependence of the ionic conductivity did not show a single Arrhenius behavior but did show a Williams–Landel–Ferry type behavior. The ionic conductivity at a reduced temperature (T_g + 90 °C) was in the range of (0.49–2.1) × 10^{-6} S cm^{-1} for the PE-2,4 complexes, depending on the incorporated salt species. The ionic conductivity at this reduced temperature for the PE-2,10 complexes was considerably lower than that observed in the PE-2,4 complexes and was 2.2 × 10^{-8} S cm^{-1} for the PE-2,10–LiSCN complex, 6.5 × 10^{-10} S cm^{-1} for the PE-2,10–NaSCN complex, and about 10^{-10} S cm^{-1} for the PE-2,10–KSCN complex. The ionic mobility estimated from the transient ionic current method was 10^{-7}–10^{-6} cm^2 V^{-1} s^{-1} at this temperature and was not affected greatly by the polymer structure and the incorporated salt species, which suggested that the free volume theory is valid for the ion transport in the polymer complexes. The lower ionic conductivity for the PE-2,10 complexes could be attributed to the lower number of carrier ions.

Introduction

Ion-conducting behavior in synthetic polymers has remained unclairified for a long time because ionic conductivity of usual polymers was extremely low and origin and kinds of carrier ions could not be exactly defined. However, relatively high ionic conductivity has recently been attained in certain kinds of ion-containing polymers.[1–10] Most of these ion-containing polymers are polymer complexes formed by host polymers and alkali metal salts. The investigation of the ionic conductivity has gradually revealed the structure–conductivity relationships in these ion-containing polymers.

We have developed the method of ionic conductivity determination by means of complex impedance measurements,[3,4,9] based on an appropriate equivalent circuit to interpret complex impedance diagrams, and have investigated structure–conductivity relationships in certain kinds of polymer complexes. Ionic conductivity, thus ob-

0024-9297/86/2219-0188$01.50/0

Chart I

PE2,4 PE2,10

Table I
Molecular Characteristics of Aliphatic Polyesters

code	(η_{sp}/C^a)/ (dL g^{-1})	GPC data			DSC data	
		$10^{-4}M_n$	$10^{-4}M_w$	M_w/M_n	T_g/°C	T_m/°C
PE-2,4	0.29	2.34	6.05	2.59	−9	103
PE-2,10	0.52	3.30	8.96	2.71	−42	79

[a] 0.1 g/10 cm^3 in chloroform at 30 °C.

tained, was influenced by many factors, such as chemical structure[3-10] and glass transition temperature (T_g) of host polymers,[6] degree of crystallinity,[5] and concentration and species of incorporated salts,[3-9] as seen in polymer complexes based on poly(ethylene succinate), poly(β-propiolactone),[5] poly(propylene oxide),[3,7-9] and poly(ethylene oxide-*co*-dimethylsiloxane).[6] Furthermore, as ionic conductivity is determined by the product of the number of carrier ions and their mobility, it is very important that the conductivity is resolved into the number of carrier ions and their mobility and that the effects of these factors on both components are investigated. From this point of view, we have also developed the method of ionic mobility determination by means of isothermal transient ionic current measurements.[7,8,10] This method was successful for the direct determination of the ionic mobility of main charge carriers[7,8] and in some cases successful for the determination of ionic mobilities of both cation and anion, thus allowing determination of the ionic transference number.[10]

This article deals with the effects of polymer structure and incorporated salt species on the ionic conductivity of polymer complexes formed by aliphatic polyester and alkali metal thiocyanate (LiSCN, NaSCN, and KSCN). Poly(ethylene succinate) (PE-2,4) and poly(ethylene sebacate) (PE-2,10) were selected as the host polymers. These effects are discussed in terms of carrier mobility and the number of carrier ions in these polymeric media.

Experimental Section

A. Preparation of Polymer Complexes. PE-2,4 and PE-2,10 were synthesized by melt polycondensation of dimethyl succinate and dimethyl sebacate with ethylene glycol, respectively. Precise conditions for the synthesis of PE-2,4 are described elsewhere.[4] PE-2,10 was synthesized according to the same method as PE-2,4. The characteristics of the polyesters obtained are summarized in Table I. LiSCN, NaSCN, and KSCN were dried under reduced pressure (10^{-3} torr) at 150 °C for 8 h before use.

Weighed amounts of the polyester and the salt were mixed and heated under a dry nitrogen stream at 120 °C for the PE-2,4 system and at 90 °C for the PE-2,10 system. The molar ratio of the salt to the repeat unit of the polyesters was kept at 0.08. After the sample became transparent, it was cooled to room temperature to yield crystalline polymer complexes and was crushed to a fine powder. This procedure was repeated twice. The polymer complexes obtained were annealed under vacuum at 60 °C for 24 h to reach an equilibrium crystallization. Standard inert-atmosphere techniques within an argon-filled drybox were used during the preparation of the complexes in order to exclude traces of water.

B. Methods. The polymer complex was pressed into cylindrical pellets (13-mm diameter, about 0.3-mm thickness). The pellet was sandwiched between platinum electrodes (13-mm diameter) and packed in a sealed cell with stainless steel terminals, which were connected to the measuring device. Cell assembly was carried out under an inert atmosphere within the drybox.

The complex impedance method was used in order to estimate the ionic conductivity of the polymer complex. Frequency dependence of the cell impedance was measured over the frequency range 5 Hz to 500 kHz. Bulk resistance was estimated from the corresponding component of an equivalent circuit required to account for the impedance spectrum, as shown in earlier articles.[3,4] The isothermal transient ionic current method[7,10-13] was used to measure the mobility of ionic carriers. The electric circuit for this measurements is shown elsewhere.[10] The transient current through the cell with first application of a step voltage and that after applying a step voltage for an appropriate time and reversal of the applied voltage polarity were recorded. The measurements were carried out several times.

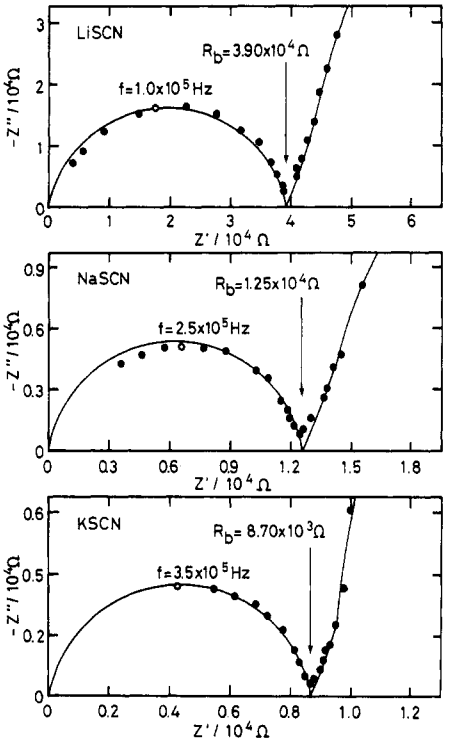

Figure 1. Complex imdedance diagrams for PE-2,4 complexes sandwiched between platinum electrodes at 70 °C.

Average molecular weights of the polyesters were measured with a Waters Associate 150C gel permeation chromatograph (GPC) with a RI detector at 100 °C, by using *m*-cresol as a carrier solvent. Narrow-distribution polystyrenes were used as the elution standards. Differential scanning calorimetry (DSC) was carried out on a Rigaku Denki 8085 DSC apparatus at a heating rate of 20 °C min^{-1}. X-ray diffraction patterns were measured with a Rigaku Denki RAD-IIA X-ray diffractometer by using a Ni-filtered Cu Kα line.

Results and Discussion

A. Temperature Dependence of Ionic Conductivity. X-ray diffraction patterns (2θ = 3–40°) of the salt-free polyesters, which had the same thermal history as the polymer complexes, showed that both polyesters were partially crystalline polymers. The polymer complexes showed diffraction peaks at the same position as the host polymers, and no diffraction peaks assignable to the incorporated salts were observed. Thus, it was suggested that the incorporated salts were dissolved in the amorphous region of the host polymers. Melting points (DSC) of the polymer complexes were independent of the incorporated salt species and were 96 °C for the PE-2,4 complexes and 76 °C for the PE-2,10 complexes. The enthalpy of melting for the host polymers was 93 cal g^{-1} for PE-2,4 and 39 cal g^{-1} for PE-2,10. The enthalpy for the polymer complexes were somewhat lower and were 65–75% of those for the host polymers, independent of the incorporated salt species.

Figure 1 shows typical complex impedance diagrams for the PE-2,4 complexes. The general profile of the impedance diagrams was an arc with a spur. The low-frequency spur is based on the interfacial impedance between the

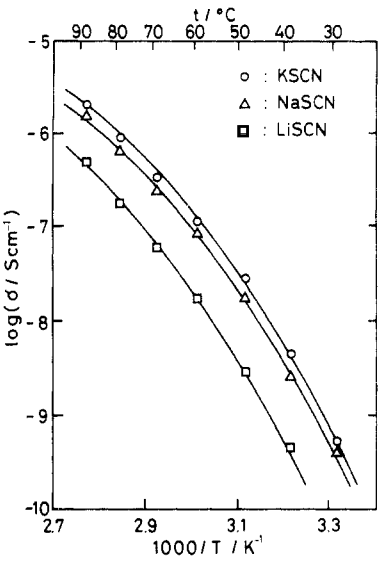

Figure 2. Temperature dependence of ionic conductivity for PE-2,4 complexes. The conductivity was calculated from the bulk resistance found in the complex impedance diagrams.

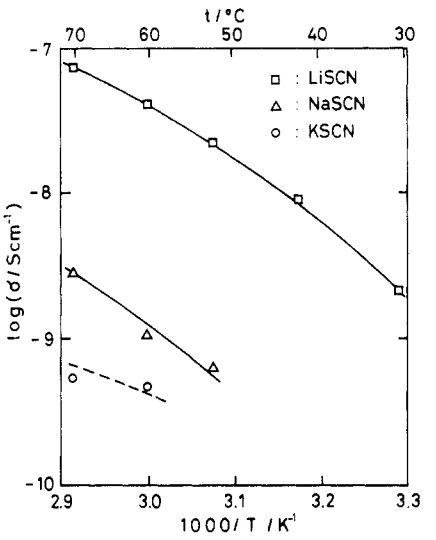

Figure 3. Temperature dependence of ionic conductivity for PE-2,10 complexes. The conductivity was calculated from the bulk resistance found in the complex impedance diagrams.

complex and the electrodes, interpreted by the equivalent circuit of the parallel combination of interfacial resistance and interfacial capacity in series with bulk resistance.[4] The high-frequency arc is based on the bulk impedance, interpreted by the equivalent circuit of the parallel combination of the bulk resistance and geometrical capacity.[4] Thus, the resistances shown in the figure correspond to the bulk resistances (R_b) of the samples. The profile of the low-frequency spur indicates that platinum is an ion-blocking electrode toward the complexes. The impedance diagrams for the PE-2,10 were similar to those for the PE-2,4 complexes. However, the impedance values were considereably higher than those of the PE-2,4 complexes.

Figure 2 shows the temperature dependence of the ionic conductivity for the PE-2,4 complexes. The conductivity was calculated from the R_b values found in the complex impedance diagrams. If a comparison of the conductivity was made at the same temperature, the magnitude of the conductivity followed the order PE-2,4–KSCN, PE-2,4–NaSCN, and PE-2,4–LiSCN complexes. The temperature dependence of the ionic conductivity did not show a single Arrhenius behavior but did show a Williams–Landel–Ferry type behavior.[14] Since the incorporated salts were dissolved in the amorphous region of PE-2,4 and T_g's of the complexes lay below the measuring temperature range, this Williams–Landel–Ferry type behavior suggests the cooperative motion of carrier ions with a micro-Brownian motion of the polymer backbone.

Figure 3 shows the temperature dependence of the ionic conductivity for the PE-2,10 complexes. The conductivity was also calculated from the R_b values in the complex impedance diagrams. As for the PE-2,10–KSCN complex, the R_b values were estimated as the intersections of the extrapolated arcs of the bulk impedance (by a microcomputer) with the Z' axis, since measurable impedance loci were limited to a high-frequency part of the bulk impedance arcs. In contrast to the conductivity results of the PE-2,4 complexes (Figure 2), the magnitude of the conductivity for the PE-2,10 complexes at the same temperature followed the order PE-2,10–LiSCN, PE-2,10–NaSCN, and PE-2,10–KSCN complexes. Furthermore, the conductivity of the PE-2,10–LiSCN complex was comparable to that of the Pe-2,4 complexes, whereas the conductivities of the PE-2,10–NaSCN and PE-2,10–KSCN complexes were lower than that of the PE-2,10–LiSCN complex by a factor of $10–10^2$. The temperature dependences did not result in straight lines but in bent curves, as seen in the PE-2,4 complexes.

B. Analysis of Effects of Polymer Structure and Salt Species on Ionic Conductivity. The ionic conductivity of the polymer complexes was affected greatly by the polymer structure and the incorporated salt species. Since ionic conductivity is determined by the product of the number of carrier ions and their mobility, the different conductivity values arise from the differences in the number of carrier ions and/or their mobility.

The temperature dependence of the ionic conductivity showed the Williams–Landel–Ferry type behavior, as seen in Figures 2 and 3. Thus, we considered that the mechanism of ion transport might be explained by the free volume theory. We have presented the equation[7] that expressed the temperature dependence of the ionic conductivity in the rubbery state for this kind of ionic conductor containing a monovalent salt. The equation is

$$\sigma = \frac{e^2 D_0 N_0}{kT} \exp\left[-\frac{U/2\epsilon}{kT} - \frac{\gamma V_i^*}{V_g(f_g + \alpha(T - T_g))} \right] \quad (1)$$

where e is elementary electric charge, N_0 and D_0 are constants, k is the Boltzmann constant, U is the lattice energy for the incorporated salt, ϵ is the relative dielectric constant of the complex, γ is a numerical factor, V_i^* is the critical volume required for the ionic migration, V_g is the specific volume at T_g, f_g is the fractional free volume at T_g, and α is the expansion coefficient of the free volume. The first and second terms in the exponential of eq 1 correspond to the Arrhenius activation process for carrier generation and the free volume process for carrier mobility, respectively. In order to confirm the validity of the free volume theory for the ionic migration, we tried to estimate the ionic mobility at a constant reduced temperature ($T - T_g$) from the transient ionic current method.[10] If ionic migration is explained by the free volume theory, the ionic mobility at a constant ($T - T_g$) may be almost independent of the polymer structure and of the incorporated salt species because the main influencing term on the ionic mobility is ($T - T_g$).

Figure 4a shows the typical time dependence of current through the PE-2,4 complexes sandwiched between platinum electrodes with the first application of a step voltage (3.0 V) at T_g + 90 °C. This temperature was selected in

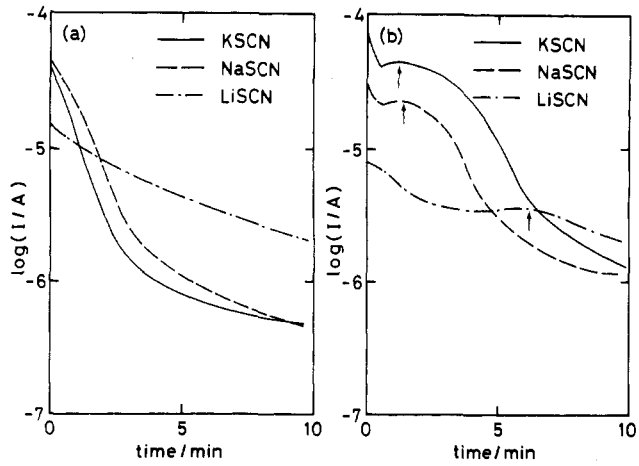

Figure 4. Time dependence of current through PE-2,4 complexes sandwiched between platinum electrodes: (a) with first application of a step voltage (3.0 V) and (b) after applying the constant voltage for 120 min and reversing the applied voltage polarity.

order to make the current levels of both complexes high enough to ensure their reliability. The current initially decreased rapidly and continued to decrease gradually to reach current levels after 10 min lower than the initial ones by one or two orders of magnitude. Since platinum is a nonblocking electrode for electrons but a blocking electrode for the ions, as seen in the complex impedance diagrams, this large decrease implies that this current is based on the migration of ions. Furthermore, current through the salt-free PE-2,4 was far lower than through the complexes and was of the order of 10^{-9} A at 87 °C. Thus, this current can be attributed to the migration of ions originating from the incorporated salts. When the time dependence of the current is dominated by the migration of ions, the current through the complex with ion-blocking electrodes can be expressed by

$$I(t) = (S/d)V^*(t)\sum[n(t)e\mu] \quad (2)$$

where S and d are sample area and thickness, respectively, $V^*(t)$ is an effective voltage across the sample, $n(t)$ is the number of ionic carriers in the bulk, and μ is the ionic mobility. Thus the profile of the transient ionic current can be explained by the time dependence of the terms $V^*(t)$ and $n(t)$. $V^*(t)$ may decrease with time and may deviate from the applied voltage (V) because of the formation of space charge in the vicinity of the electrodes. $n(t)$ may also decrease with time because of the cleanup effect of the carrier ions in the bulk. If we assume that $V^*(t)$ is consistent with V for the initial short time and that there is one kind of mobile species, eq 2 reduces to

$$I(t) = \frac{Sn_0e\mu_iV}{d}\exp\left[-\left(\frac{\mu_iV}{d^2}\right)t\right] \quad (3)$$

where n_0 is the number of carrier ions at $t = 0$. Thus, we estimated the ionic mobility (μ_i) from the initial slope of the transient ionic current.

Figure 4b shows the typical transient ionic current of the PE-2,4 complexes after applying 3.0 V dc for 120 min in one direction and reversing the applied voltage polarity. The current profile was considerably different from that with the first voltage application seen in Figure 4a. The time dependence of the current showed a maximum (indicated by an arrow in the figure) at a given time. For these polarity reversal experiments, we may have the following situation. Before reversal of the applied voltage polarity, the carrier ions that cannot discharge at the electrode accumulate in the vicinity of the electrode. After the reversal, the number of carrier ions in the bulk increases by the release of the ions from the accumulated layer. Just after the carrier ions reach the opposite electrode, the accumulation of the carrier ions begins again, resulting in a decrease in the number of carrier ions. Thus, the number of carrier ions in the bulk reaches a maximum at the current-maximum time (τ). As a result, τ coincides with the time-of-flight of carrier ions from one electrode to the other. Between $t = 0$ and $t = \tau$, $V^*(t)$ may change due to the space-charge effects. For instance, $V^*(0)$ is higher than V, and $V^*(\tau)$ is lower than V. We assume here that the average $V^*(t)$ between $t = 0$ and $t = \tau$ is equal to V as a first approximation. On this assumption, the carrier mobility (μ_τ) can be calculated by

$$\mu_\tau = d^2/(\tau V) \quad (4)$$

Table II
Conduction Parameters of Polymer Complexes at T_g + 90 °C

host polym	salt	T_g/°C	σ/(S cm^{-1})	μ_i/(cm^2 V^{-1} s^{-1})	μ_τ/(cm^2 V^{-1} s^{-1})
PE-2,4	LiSCN	−3	4.9×10^{-7}	1.3×10^{-6}	2.7×10^{-6}
PE-2,4	NaSCN	−3	1.7×10^{-6}	2.6×10^{-6}	5.7×10^{-6}
PE-2,4	KSCN	−3	2.1×10^{-6}	4.6×10^{-6}	5.2×10^{-6}
PE-2,10	LiSCN	−37	2.2×10^{-8}	5.7×10^{-7}	2.0×10^{-6}
PE-2,10	NaSCN	−37	6.5×10^{-10}	3.0×10^{-7}	8.8×10^{-7}
PE-2,10	KSCN	−42	$\simeq 10^{-10}$		

Table II shows the conduction parameters, including the ionic conductivity and the mobility of carrier ions, for the polymer complexes at T_g + 90 °C. The mobility values (μ_i and μ_τ) were averages of the experimental results carried out several times at different applied voltages. The ionic current in the PE-2,10–KSCN complex was too low to define the ionic mobility. The mobility values estimated by both methods agree reasonably well with each other. In the case of the PE-2,4–LiSCN complex, it has been demonstrated that the transference number of Li^+ ions is close to unity.[10] Thus, the μ_i and μ_τ values represent the mobility of Li^+ ions. Since the main charge-carrier species for the other complexes could not be specified, we can only say here that the mobility values in Table II are those for the main charge carriers in each complex. The ionic mobilities for the PE-2,4 complexes were similar and were of the order of 10^{-6} cm^2 V^{-1} s^{-1} at this reduced temperature. This may imply that the free volume theory is valid for the mechanism of ion transport. Since the difference of the ionic mobility depending on the incorporated salt species was not so clear, we could not define which is the more important factor on the difference in conductivity, the difference in the carrier mobility or that in the number of carrier ions. The carrier mobilities for the PE-2,10 complexes were somewhat lower, compared with those for the PE-2,4 complexes. However, this difference seemed to be negligible when one noticed the considerably lower conductivity for the PE-2,10 complexes. Thus ion transport in the PE-2,10 complexes may also obey the free volume mechanism. The lower conductivity for the PE-2,10 complexes at this reduced temperature may be due to lower number of carrier ions. Furthermore, it should be noted that the large difference in conductivity for both complexes was not reflected in the mobility difference.

The incorporated salt (MX) seems to be dissolved in the host polymer in the following manner:

$$M^+{\cdot}X^- \rightleftarrows M^+ + X^- \quad (5)$$

A part of the incorporated salt may dissociate to free ions, which function as carrier ions. For the ion dissociation in polymeric media, solvation of an ion with polar groups in

the polymer backbone may be an essential process. There are two possible processes for the solvation in polymeric media: one is the solvation by intrapolymer polar groups and the other is that by interpolymer polar groups. The former process may involve the cooperative interaction of the neighboring polar groups in the polymer backbone with an ion. We considered that the former process was more important for the carrier generation in polymeric media. The polar groups in PE-2,4 exist in high density, whereas those in PE-2,10 are far separated by octamethylene units. Thus, PE-2,4 may favor the former process. In contrast, PE-2,10 does not favor the former process because of the entropical instability. Thus, the ion dissociation in PE-2,10 may be suppressed, especially in the NaSCN and KSCN complexes, which may be responsible for the lower ionic conductivity.

References and Notes

(1) Wright, P. V. *Br. Polym. J.* **1975**, *7*, 319.
(2) Armand, M. B.; Chabagno, J. M.; Duclot, M. J. In "Fast Ion Transport in Solid"; Vashishta, P., Mundy, J. N., Shenoy, G. K., Eds.; North-Holland: Amsterdam, 1979; pp 131-136.
(3) Watanabe, M.; Sanui, K.; Ogata, N.; Inoue, F.; Kobayashi, T.; Ohtaki, Z. *Polym. J. (Tokyo)* **1984**, *16*, 711.
(4) Watanabe, M.; Rikukawa, M.; Sanui, K.; Ogata, N.; Kato, H.; Kobayashi, T.; Ohtaki, Z. *Macromolecules* **1984**, *17*, 2902.
(5) Watanabe, M.; Togo, M.; Sanui, K.; Ogata, N.; Kobayashi, T.; Ohtaki, Z. *Macromolecules* **1984**, *17*, 2908.
(6) Nagaoka, K.; Naruse, H.; Shinohara, I.; Watanabe, M. *J. Polym. Sci., Polym. Lett. Ed.* **1984**, *22*, 659.
(7) Watanabe, M.; Sanui, K.; Ogata, N.; Kobayashi, T.; Ohtaki, Z. *J. Appl. Phys.* **1985**, *57*, 123.
(8) Watanabe, M.; Sanui, K.; Ogata, N.; Inoue, F.; Kobayashi, T.; Ohtaki, Z. *Polym. J. (Tokyo)* **1985**, *17*, 549.
(9) Watanabe, M.; Oohashi, S.; Sanui, K.; Ogata, N.; Kobayashi, T.; Ohtaki, Z. *Macromolecules* **1985**, *18*, 1945.
(10) Watanabe, M.; Rikukawa, M.; Sanui, K.; Ogata, N. *J. Appl. Phys.* **1985**, *58*, 736.
(11) Stagg, J. P. *Appl. Phys. Lett.* **1977**, *31*, 532.
(12) Greeuw, G.; Verwey, J. F. *J. Appl. Phys.* **1984**, *56*, 2218.
(13) Kosaki, M.; Ohshima, H.; Ieda, M. *J. Phys. Soc. Jpn.* **1970**, *29*, 1012.
(14) Williams, M. L.; Landel, R. F.; Ferry, J. D. *J. Am. Chem. Soc.* **1955**, *77*, 3701.

Binding Sites of Cu^{2+} in Chitin and Chitosan. An Electron Spin Resonance Study

Shulamith Schlick

Department of Chemistry, University of Detroit, Detroit, Michigan 48221.
Received March 15, 1985

ABSTRACT: X-band ESR spectra of copper at high dilution in chitin and chitosan were measured at 77 and 297 K. Two bonding sites for Cu^{2+} in chitin were observed. Site 1, with $g_{\parallel}^{(1)} = 2.244$, $g_{\perp}^{(1)} = 2.069$, $A_{\parallel}^{(1)} = 188 \times 10^4$ cm^{-1}, and $A_{\perp}^{(1)} = 30 \times 10^{-4}$ cm^{-1} at 77 K, is dominant. Site 2 has approximately the same values of $g_{\perp}$ and $A_{\perp}$ as site 1 but $g_{\parallel}^{(2)} = 2.327$ and $A_{\parallel}^{(2)} = 162 \times 10^{-4}$ cm^{-1} at 77 K. One bonding site for Cu^{2+} in chitosan was observed, identical with site 1 in chitin. Analysis of the ESR parameters suggests that site 1 represents a square-planar arrangement of four nitrogen ligands around Cu^{2+}, while site 2 represents a tetrahedrally distorted structure of three N and one O *or* two N and two O ligands. Examination of the crystal structure of α-chitin suggests that a site consisting of two N and two O ligands is more probable. In both chitin and chitosan the suggested structures imply that modification of interchain distances occurs on chelation.

Introduction

Chitin is a naturally occurring polymer of the formula poly[(1→4)-*N*-acetyl-β-D-glucosamine], and chitosan is the corresponding N-deacetylated compound. The theoretical nitrogen percent is 6.89 in chitin and 8.70 in the completely deacetylated chitosan. In practice, because deacetylation is usually incomplete, chitin and chitosan represent a range of compounds with varying nitrogen content between the above limits. The ability of these compounds to bind selectively metal ions has been recognized for some time.[1] While the ability of chitin and chitosan to retain alkali and alkaline earth metal ions is extremely low, most transition-metal ions of the first row are strongly chelated, with zinc, nickel, and copper strongly and selectively favored.

Copper chelation has been studied extensively as a function of temperature, pH, time of contact with the metal solutions, and various degrees of chitin deacetylation[2,3] and polymer crystallinity. It was found that the chelating ability of chitosan is much greater than that of chitin, a result that has been associated with the higher amino group content in chitosan. Plots of percent copper ion collection vs. amino group content in chitosans with various degrees of deacetylation did not indicate a linear relationship, suggesting that other factors affect the ion binding.[3b] The role of the active hydroxy groups at the C_3 and C_6 positions in the chelation process is evident in a study that shows that the binding of copper and iron ions is reduced in chitin by methylation or acetylation.[4] Some evidence has been presented that more than one active binding site exists.[1,5] This conclusion was based on the fact that adsorption of a metal by chitin and chitosan from mixed-metal solutions was not proportional to the metal concentration in solution. No specific binding scheme or geometry was deduced or suggested in these studies.[5]

The purpose of this study is to obtain structural information on the metal ion ligation in chitin and chitosan using the technique of electron spin resonance (ESR). In many cases, ESR parameters of paramagnetic ions have been interpreted in terms of ligation to specific atoms in a variety of complexes, including complicated biological systems.[6-9] In this study we have detected for Cu^{2+} one binding site in chitosan and two binding sites in chitin. Specific coordination around the metal ion is suggested for each site.

Experimental Section

Chitin purified from crustacean shells and chitosan from crustacean chitin were obtained from Calbiochem-Behring Corp. of La Jolla, CA. Copper chelation was obtained by mixing a suspension of 0.1 g of chitin or chitosan in 20 cm^3 of D_2O and adding $CuSO_4 \cdot 5H_2O$ to an approximate molar ratio of 1/100 for Cu to monomeric chitin or chitosan. The suspension was stirred for 24 h, filtered, rinsed with D_2O, dried, and kept in a desiccator.[10]

0024-9297/86/2219-0192$01.50/0